J Mater Sci (2009) 44:1934–1951
DOI 10.1007/s10853-009-3262-9

REVIEW

Ceramic matrix composites containing carbon nanotubes

Johann Cho · Aldo R. Boccaccini · Milo S. P. Shaffer

Received: 3 November 2008 / Accepted: 8 January 2009 / Published online: 28 February 2009

Abstract Due to the remarkable physical and mechanical properties of individual, perfect carbon nanotubes (CNTs), they are considered to be one of the most promising new reinforcements for structural composites. Their impressive electrical and thermal properties also suggest opportunities for multifunctional applications. In the context of inorganic matrix composites, researchers have particularly focussed on CNTs as toughening elements to overcome the intrinsic brittleness of the ceramic or glass material. Although there are now a number of studies published in the literature, these inorganic systems have received much less attention than CNT/polymer matrix composites. This paper reviews the current status of the research and development of CNT-loaded ceramic matrix composite (CMC) materials. It includes a summary of the key issues related to the optimisation of CNT-based composites, with particular reference to brittle matrices and provides an overview of the processing techniques developed to optimise dispersion quality, interfaces, and density. The properties of the various composite systems are discussed, with an emphasis on toughness; a comprehensive comparative summary is provided, together with a discussion of the possible toughening mechanism that may operate. Last, a range of potential applications are discussed, concluding with a discussion of the scope for future developments in the field.

J. Cho · A. R. Boccaccini (✉)
Department of Materials, Imperial College London,
London SW7 2BP, UK
e-mail: a.boccaccini@imperial.ac.uk

J. Cho · M. S. P. Shaffer (✉)
Department of Chemistry, Imperial College London,
London SW7 2AZ, UK
e-mail: m.shaffer@imperial.ac.uk

Introduction

Ceramic matrix composites (CMCs) have been developed to overcome the intrinsic brittleness and mechanical unreliability of monolithic ceramics, which are otherwise attractive for their high stiffness and strength [1]. The issue is particularly acute with glasses, as the amorphous structure does not provide any obstacle to crack propagation and the fracture toughness is very low (<1 MPa $m^{1/2}$) [2]. In addition to mechanical effects, the reinforcing phase may benefit other properties such as electrical conductivity, thermal expansion coefficient, hardness and thermal shock resistance [1, 3]. The combination of these characteristics with intrinsic advantages of ceramic materials such as high-temperature stability, high corrosion resistance, light weight and electrical insulation, makes CMCs very attractive functional and structural materials for a variety of applications; they have particular relevance under harsh conditions where other materials (e.g. metallic alloys) cannot be used effectively [4–6].

A wide range of reinforcing fibres have been explored, including those based on SiC, carbon, alumina and mullite [7–9]. However, carbon fibres are amongst the highest performance toughening elements investigated, since the first reports of their use in ceramic matrices were published in the 1960s [10]. The fracture toughness of carbon and SiC fibre reinforced glass and CMCs can be much better than that of the native matrix, as demonstrated by a wealth of available data in the literature [4–6, 10, 11] (for example, SiC fibre reinforced glass–ceramic composites can reach 17 MPa $m^{1/2}$ [5]). Various toughening mechanisms can be involved, including fibre debonding, fibre pull-out and crack bridging [11].

Carbon nanotubes (CNTs) have received an enormous degree of attention in recent years, and, in the context of

composites, they are often seen as the 'next generation' of carbon fibre. Although their remarkable properties have suggested applications as diverse as tissue scaffolds, field emission guns and supercapacitor electrodes [12], the interest in composite materials is driven by both the mechanical and functional properties that can be obtained at very low density (typically in the range 1.5–2.0 gcm^{-3}). For individual perfect CNTs, the axial stiffness has been shown to match that of the best carbon fibres (approaching around 1 TPa), whilst the strength is an order of magnitude higher (around 50 GPa) [13]. Their electronic properties depend subtly on the exact structure, but larger CNTs are essentially metallic conductors [14]; smaller CNTs can offer unique optoelectronic properties, useful, for example, in non-linear optics [15]. Ballistic electron transport effects can be related to uniquely high current carrying capacity (up to 10^9 Acm^{-2}) whilst the axial thermal conductivity is higher than that of diamond (>2,000 Wm^{-1} K^{-1}) [16]. It is worth noting that surface areas of CNTs can be very high since, in the absence of agglomeration, every atom of a single walled nanotube lies on its surface; however, this factor can be a mixed blessing when considering composite applications, as discussed further below.

One other significant characteristic of CNTs is their very high aspect (length to diameter) ratio which is relevant to load transfer with the matrix and, hence, effective reinforcement. Standard continuous-fibre composites have excellent anisotropic structural properties combined with low density, but are expensive to process and are limited to simple shapes [3]. Short-fibre composites, on the other hand, are easier to produce in complex shapes but with conventional fibres, the aspect ratio is typically limited to around 100, after processing [17]. In principle, the small absolute length of CNTs, combined with their resilience in bending, allows them to be manipulated with conventional processing equipment, potentially retaining their high aspect ratio; however, in practice, length degradation is known to occur under high shear conditions. The high aspect ratio of CNTs can also encourage the formation of percolating networks that are relevant to functional properties, particularly electrical conductivity [18]; indeed the lowest percolation threshold for any system has been observed in kinetically formed networks of CNTs in epoxy [19].

Structurally, CNTs have diameters in the range of around 1 nm to a somewhat arbitrary upper limit of 100 nm, and lengths of many microns (even centimetres in special cases) [20]. They can consist of one or more concentric graphitic cylinders, forming single or multi walled nanotubes (SWCNTs/MWCNTs). In contrast, commercial (PAN and pitch) carbon fibres are typically in the 7–20 μm diameter range, whilst vapour-grown carbon fibres (VGCFs) have a broad range of intermediate diameters. Compared to carbon fibres, the best nanotubes can have almost atomistically perfect structures; indeed, there is a general question as to whether the smallest CNTs should be regarded as very small fibres or heavy molecules, especially as the diameters of the smallest nanotubes are similar to those of common polymer molecules. Consequently, it is not yet clear to what extent conventional fibre composite understanding can be extended to CNT-composites, or whether new mechanisms will emerge.

Although the perfect CNT structure is very appealing, real materials are very diverse and vary significantly in terms of dimensions, purity, surface chemistry, crystallinity, graphitic orientation, degree of entanglement and cost. These factors directly affect the properties and processability of CNTs and they must be considered when interpreting their performance in a given application. In very broad terms, CNTs can be divided into two classes depending on the synthetic route used to prepare them. High-temperature evaporation methods, using arc-discharge [21, 22] or laser ablation [23], tend to yield highly crystalline CNTs, with low defect concentrations and good mechanical properties, but are relatively impure, containing other, unwanted carbonaceous impurities; these methods usually work on the gram scale and are, therefore, relatively expensive. On the other hand, for use in composites, large quantities of nanotubes are required at low cost, ideally without complicated purification steps. At present, only chemical vapour deposition (CVD) or catalytic growth processes [24] satisfy these requirements and, as such, are the materials of choice for composite work, both in academia and in industry [25]; a number of companies have scaled up such processes to 100 tonnes per year or more. CVD materials contain residual catalyst particles, and sometimes amorphous carbon, but are otherwise relatively pure. On the other hand, these gas-phase processes operate at lower temperatures and lead to structurally imperfect nanotubes, often with seriously reduced intrinsic properties [26]. It is worth noting that there are currently around four orders of magnitude between the prices of the most expensive and cheapest commercial nanotube products.

Over the last 10 years, interest in the application of CNTs as toughening agents in polymer, ceramic or metal matrix composites has grown rapidly. The potential of developing advanced nanocomposites that manifest, to some degree, the extraordinary properties of individual CNTs is very attractive in fields as diverse as aerospace, sports equipment, and biomedical devices [27, 28]. The vast majority of CNT composite work has focused on polymer matrices [29], whilst comparatively few investigations have explored inorganic (ceramic or glass) matrices and the potential toughening mechanisms that might be associated with CNT reinforcements. For successful CNT/composite development, a number of key challenges must be met [30]. First, CNTs with intrinsically good mechanical properties must be obtained in reasonable quantity at acceptable cost. The CNTs

must then be processed in such a way as to ensure that a homogeneous dispersion is obtained within the matrix, whilst developing an appropriate degree of interfacial bonding. These overall requirements are common to all CNT-composites, and often involve chemical surface modification of the CNTs [31]. Of course, in the case of inorganic matrix composites, an 'appropriate' interface may be defined differently [1]. In addition, obtaining a high degree of inorganic matrix densification, without damaging the CNTs, is especially challenging. The following sections address the key issues currently raised in CNT-based composites, in general, and discuss the importance of these crucial factors for successful development of ceramic and glass matrix composites containing CNTs.

Key issues in CNT-based composites

CNT dispersion in the matrix

One of the biggest challenges in processing nanotube composites lies in achieving a 'good' dispersion [32]. It is important that the individual nanotubes are distributed uniformly throughout the matrix and well-separated from each other; the presence of agglomerates is extremely undesirable, especially in ceramic matrices, as they can act as defects leading to stress-concentration, and premature failure, particularly if the matrix does not fully penetrate the agglomerate during processing. On the other hand, with a good dispersion, each nanotube is loaded individually over a maximum interfacial area, and can contribute directly to the mechanical properties and to toughening mechanisms. Figure 1a [33] and b [34] show typical microstructures of agglomerated and homogeneous CNT/glass matrix composites, respectively. CNTs have a tendency to agglomerate due to their relatively high surface areas, their high aspect ratios, and typically poor interactions with solvents or matrix components [35]. SWCNTs, in particular, tend to agglomerate into 'ropes' or 'bundles', consisting of many parallel nanotubes bound by van der Waals forces. High loading fractions favour agglomeration not only because the particles come into contact more often, but also because there can be a shortage of matrix material to 'wet out' the large surface area of the filler. It is quite a common result for nanocomposites, in general, that properties are enhanced at low loading fractions but cannot be increased further due to CNT agglomeration above a few vol.%. The situation is more ambiguous when addressing transport properties, especially electrical conductivity, as a network of touching nanotubes is desired. However, even in this case, best results may be obtained by generating a good dispersion initially, and then allowing the network to form [19, 36].

A particular practical problem is that the dispersion of high aspect ratio, nanoscale objects is very hard to quantify objectively. Characterisation usually consists of a qualitative assessment of a fracture surface studied under scanning electron microscopy (e.g. Fig. 1a). This approach is quite successful for discovering dense aggregates (typical of CNTs synthesised in the electric arc) or looser agglomerates in low volume fraction systems. However, at high loading fractions where the filler is necessarily densely packed, it is less effective, since any contacts may not lie in the fracture plane. In any case, careful selection of magnification(s) is required in order to come to a statistically significant conclusion; low magnifications are useful to show the uniformity of the dispersion over larger areas but are not always provided in publications. Optical microscopy can be a useful guide, again chiefly for low loading fractions since agglomerates tend to be on the order of microns (at least as big as the CNTs are long). Good dispersions, although very dark even at low loadings, transmit light without significant optical scattering. In order to obtain a good dispersion in the final composite, a suitable processing route needs to be obtained. Often the first step is to disperse the CNTs in a solvent, prior to mixing with a conventional ceramic powder (see the section "Powder processing"), a colloidal ceramic suspension (see the section "Colloidal processing") or sol-gel precursor (see the section "Sol-gel processing"). The primary method of dispersion is usually based on applying shear forces, using high shear mixers, ultrasonic probes, or ball

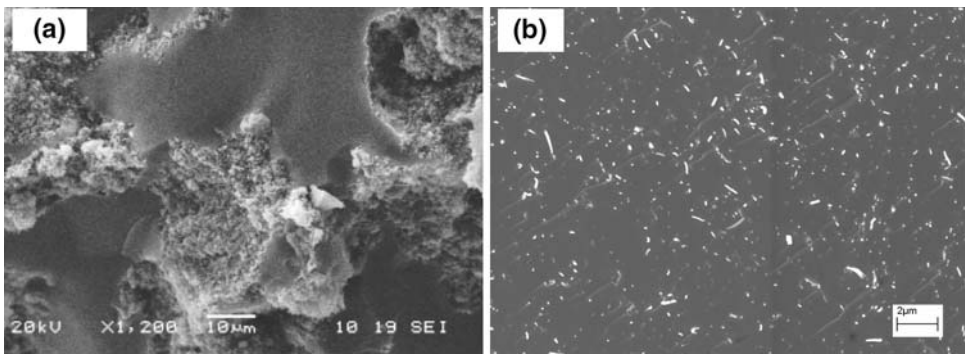

Fig. 1 SEM images of fracture surfaces of **a** agglomerated CNTs in a borosilicate glass matrix [33], and **b** homogeneously dispersed CNTs in a silica matrix (individually pull-out CNT segments can be observed which may relate to possible toughening mechanisms) [34]. Images published with permission of (**a**) Elsevier B.V., (**b**) Maney Publishing

mills. The CNT surface is often modified, either by direct functionalisation chemistry or by the use of surfactants, in order to add stability in a given solvent or to improve compatibility with a given matrix (precursor). Alternatives to the basic disperse-and-mix strategy include synthesising CNTs on the surface of ceramic particles or within pre-defined pores (see the section "In situ growth of CNTs by chemical vapour decomposition (CVD)"), and electrophoretically driven deposition (see the section "Electrophoretic deposition").

Interface engineering

In the light of the experience with conventional fibre composites, it is clear that the interfacial bonding between the CNTs and the inorganic matrix will be crucial. However, the consequences of reducing the reinforcing fibres diameter by several orders of magnitude is less obvious, and further studies of the scaling behaviour of different toughening mechanisms are required. It is possible both that the energy dissipation during fracture propagation due to familiar mechanisms such as pullout, crack deflection and crack bridging could be enhanced [37] and that new mechanisms may come into play. It seems likely that CNT-containing ceramic matrix nanocomposites should follow the example of their fibre-reinforced conventional cousins; interfaces should be of intermediate strength to maximise the energy involved in debonding the CNTs from the matrix at the same time as maintaining effective interfacial load transfer. In the case of poor or absent interfacial bonding, CNTs may even act as a source of microcracks, leading to failure. In the case of polymer/CNT-composites, interfacial adhesion is readily modified by organic surface chemistry. Such approaches can be useful during the processing of inorganic matrix composites. For example, Fig. 2 highlights intimate interface between amorphous SiO_2 and modified-MWCNTs produced by a sol-gel method [38]. However, in most ceramic systems, the high temperatures required for consolidation (see the section "Advanced consolidation techniques") removes any organic functional groups that might have been introduced to aid processing. The interface is then dominated by the direct interaction (or reaction) between the matrix and the graphitic CNT surface.

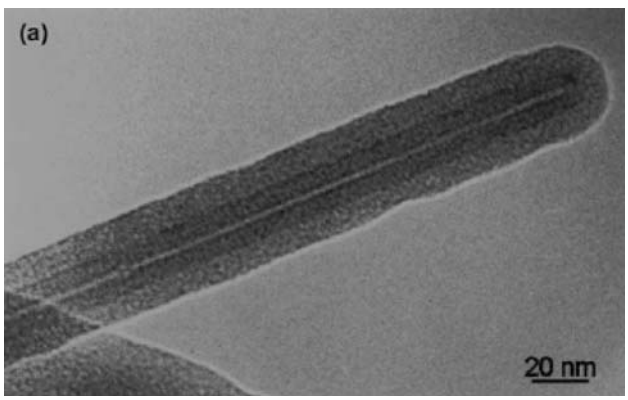

Fig. 2 TEM image of SiO_x-coated MWCNTs produced by a sol-gel method, showing a uniform silica layer, 10 nm thick [38]. Image published with permission of Elsevier B.V.

Overview of CNT/inorganic matrix composite fabrication methods

In situ growth of CNTs by chemical vapour decomposition (CVD)

One of the first studies on direct synthesis of CNT/ceramic composites (published in two parts) was authored by Peigney and co-workers [39, 40]. They have developed CVD techniques to synthesise CNTs, in situ, in the presence of the ceramic powders destined to form the matrix. CNT/metal-oxide powders can be synthesised by passing CH_4:H_2 mixtures over dispersions of transition-metal catalysts supported on oxide powders (typical combinations include Fe, Co or Fe/Co alloys on Al_2O_3, MgO or Mg Al_2O_4) [41–48]. These composite powders can then be hot pressed to form macroscopic composites. The incorporation of the long nanotube bundles grown in situ, however, has not yet been shown to provide the expected improvement in mechanical properties. The fracture strength and toughness of the CNT-containing composites developed by this method are generally lower than those of the monolithic metal-oxide composites probably due to relative low density (87–93%), as shown in Fig. 3a [41]. Although the CNTs are uniformly grown over the surface of the oxide particles, they do not end up uniformly dispersed through the volume of the final composite. On the other hand, the CNTs can be aligned using high-temperature extrusion, and the resulting materials exhibit a marked anisotropy of the electrical conductivity [45]. Interestingly, the CNTs apparently aid super-plastic forming of the composite material, an advantage attributed to inhibited matrix grain growth and grain-boundary lubrication [45]. Related studies of the preparation of CNTs/alumina composites using the in situ method have been performed by An et al. [49] & Lim et al. [50]. As discussed further below, the tribological properties were significantly improved by the presence of CNTs at the alumina grain boundaries (see Fig. 3b) [49].

A highly ordered array of parallel MWCNTs in an alumina matrix was fabricated by Xia et al. [51–53] using a variant of the in situ CVD method. The oxide support, in this case, was an amorphous nanoporous (anodised) alumina matrix with thickness 20 μm and a hexagonal array of

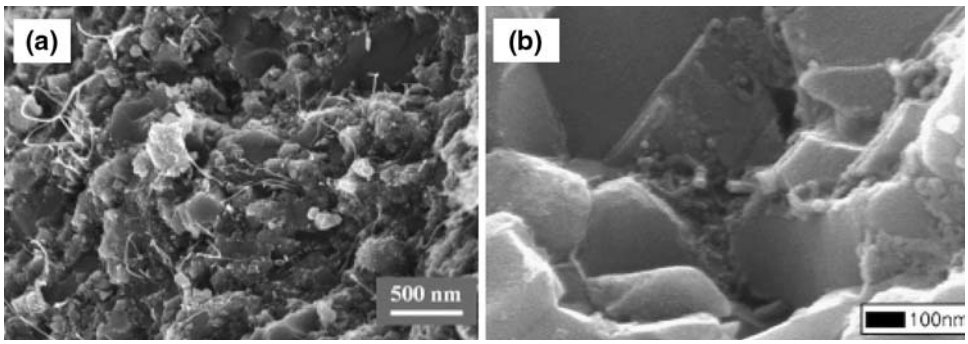

Fig. 3 SEM images showing **a** relatively well-distributed CNT network between the alumina grains [41] and **b** fracture surface morphologies of hot-pressed alumina composites containing 12.5 wt% CNT [49]. Images published with permission of Elsevier B.V.

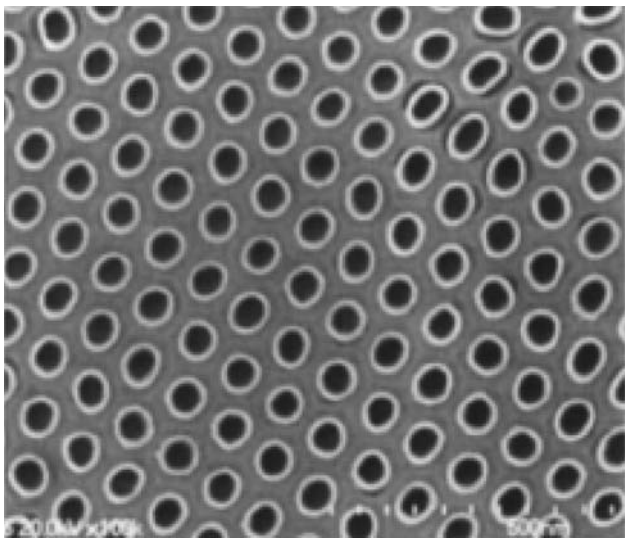

Fig. 4 SEM image of a CNT/Al_2O_3 composite by Xia et al. [51] viewed from the top. Image published with permission of Elsevier B.V.

straight pores around 30–40 nm in diameter; Co or Ni metal particles were deposited within the pores in order to catalyse the CVD growth of MWCNTs up the pore walls, creating a highly ordered unidirectional CNT CMC [51] (see Fig. 4). The authors demonstrated that the nanocomposites exhibit the three hallmarks of toughening found in micron-scale fibre composites: crack deflection at the CNT matrix interface, crack bridging by CNTs, and CNT pull-out on the fracture surfaces. The same group also combined analytical and numerical models, using cohesive zone models for both matrix cracking and nanotube crack bridging, to interpret indentation results and evaluate the fracture toughness [52] and tribological behaviour [53] of the composites.

The in situ formation of CNTs by spray pyrolysis provides a simplified one-step embodiment of the CVD method, without a separate catalyst loading/preparation step. In this case, a slurry of ferrocene (metal catalysts) and alumina nanoparticles in xylene (hydrocarbon source) is sprayed into a furnace at 1,000 °C under Ar atmosphere [54]; a similar reaction has also been explored using a SiC support [55]. The technique produces flake-like mixtures, with a heterogeneous distribution of CNTs, particularly in the through-thickness direction.

In general, the in situ growth of CNTs in ceramic matrices is an attractive processing route to synthesise composites with reasonably distributed networks of CNTs. It is relatively simple and scalable, and can be applied to a wide range of matrices, including SiC [56], TiN [57, 58], Fe_2 N [57] and $BaTiO_3$ [59–62]. However, a number of difficulties remain to be resolved. First, the synthesis process intrinsically involves the presence of metal catalysts and often leads to the deposition of amorphous carbon, particularly on the exposed oxide particle surfaces; these phases are generally undesirable in the final composite, but can be difficult to remove. Second, these in situ composites typically have relatively low density after sintering suggesting unfavourable interactions between CNTs and the matrix materials; the network of CNTs at the oxide particle surface may then form a barrier to effective sintering and the CNTs are not readily distributed into the bulk. In this approach, there is little opportunity to manipulate the interface properties to improve the outcome; rather the interface properties remain highly dependent on the particular system. Although this type of microstructure, with the CNTs at the grain boundaries, may be beneficial for certain functional or processing-related properties, it is less appealing for straight forward mechanical reinforcement.

Powder processing

Powder processing methods are very commonly applied in ceramic systems and were the first techniques considered during the early stages of the CNT/ceramic composite fabrication. Results have usually shown that conventional powder processing is not an effective means to disperse CNTs homogenously in ceramic or glass matrices; as in the case of the in situ methods discussed above, there is no driving force to distribute the CNTs from the powder particle surface into the bulk.

Powder processing is usually carried out by mixing raw CNTs and ceramic particles under wet conditions, followed

by ultrasonication and/or ball milling; the dried powder is then crushed and sieved, and finally densified by hot-pressing (HPS). Powder processing has been applied to various composites systems including borosilicate glass [33, 63], silicon nitride [64–69] alumina, [70, 71], mullite [72] and silica [73] matrix composites containing different concentrations of CNTs (typically 1–10 vol.%). These investigations have been of mixed success in terms of the quality of the microstructure homogeneity and properties achieved (see the section "Mechanical properties and possible toughening mechanisms").

Colloidal processing

There is a growing interest in using ceramic particles with similar diameters to the nanotubes to create an intimate dispersion. By adjusting the surface chemistry of the colloidal suspensions and selecting proper processing conditions, the nanoparticles can be encouraged to coat the CNTs. The coatings then screen the undesirable attractive interactions between the nanotubes, preventing agglomeration and facilitating the production of well-dispersed composites. It is worth noting that dispersion of CNTs is established by manipulating the surface chemistry of the two phases during low-temperature processing, and that this dispersion is then retained after sintering. The coating process is generally carried out by so-called heterocoagulation of nanoparticles. The heterocoagulation occurs when two (usually electrostatically) stabilised suspensions (of CNTs and matrix particles) are mixed; by ensuring that the two sets of particles have opposite charge, the coating process can be encouraged.

Perfect CNTs are intrinsically inert with minimal surface charge; in practice, as-produced CNTs, especially commercial CVD materials, have a degree of surface functionalisation, often with oxygen, but dispersibility usually remains poor. Samples are generally aggregated or entangled, and may contain impurities such as amorphous carbon or catalytic metal particles. A post-synthesis chemical treatment is frequently employed to purify and disperse the CNTs in a suitable solvent. Commonly, CNTs are oxidised in a mixture of concentrated nitric and sulphuric acids to simultaneously purify, shorten, and functionalize them [74]. These aggressive conditions attack defect sites in the CNTs, cutting them, and decorating their surface with carboxylic acid and other oxygen-containing groups. These acidic groups electrostatically stabilize the CNTs in water, or other polar liquids, by developing a negative surface charge. Similar effects occur for both MWCNTs [74] and SWCNTs [75]. The resulting electrostatic repulsion amongst the CNTs leads to a remarkable increase in the stability of the colloidal suspension [76]. In addition, functional groups on CNT surfaces can be useful sites for further chemical modification. Similarly, functionalised CNTs can be produced using other liquid-phase oxidants as well as simple thermal treatments in air or other oxidising gases. Combinations of gas and liquid phase treatments are often used in order to optimise the purification and modification process [27].

Organic surfactants or dispersants can be also used to tailor surface properties of both CNTs and ceramic particles; entangled or bundled CNTs are often dispersed in surfactant solutions using ultrasound. The effective surface charge can be manipulated from positive to negative by using cationic or anionic surfactants, respectively. Typical cationic surfactants include poly ethylene amine (PEI) [77–79] and cetyltrimethylammonium bromide (CTAB) [80, 81], whilst common anionic surfactants include PAA (polyacrylic acid) [77, 78], SDS (sodium dodecyl sulphate) [79, 82] and sodium dodecyl benzyl sulphonate (SDBS) [83]. In general, the surface charge on both the CNTs and a given type of ceramic particle can be altered on demand by employing different organic surfactants or dispersants. On the whole, the surfactants will be removed during sintering; however, they do have the potential to introduce undesirable impurities, since the inclusion of CNTs precludes a strongly oxidising calcination step.

As an example, Sun et al. [77] employed surfactants to encourage alumina particles to coat CNTs during a heterocoagulation process. The effective surface charge of both CNTs (modified with PEI) and alumina nanoparticles (modified with PAA) was established using zeta potential measurements. As expected, cationic type dispersants caused the isoelectric point (pH_{iep}) to move to a higher pH value, while anionic types move pH_{iep} to lower values. A typical TEM image of heterocoagulated CNTs and alumina particles is shown in Fig. 5a [77]. The same group [79] also used acid-treated CNTs that were subsequently heat-treated in N_2 or NH_3 to remove the carboxylic functional groups; this treatment shifted the isoelectric point of the nanotubes to a higher pH value so that their positive surface charge would be maintained (in conjunction with the addition of PEI) over a much wider pH range. These modified CNTs were mixed with negatively-charged TiO_2 nanoparticles to produce heterocoagulated powder as shown in Fig. 5b [84]. Although the overall process appears successful, the individual SWCNTs were not, apparently, debundled.

Similar heterocoagulation processes have been used for a range of crystalline matrices including Al_2O_3 [82, 85–91], Si_3N_4 [67] and SiO_2 [34, 81, 92–94]. Figure 6 shows individual CNTs protruding from the fracture surface of a CNT/SiO_2 composites produced by heterocoagulation and highlights the high microstructural homogeneity that can be obtained (J. Cho, Unpublished research). This simple approach can be extended to virtually any ceramic system by varying the pH and/or surfactant used to modify the

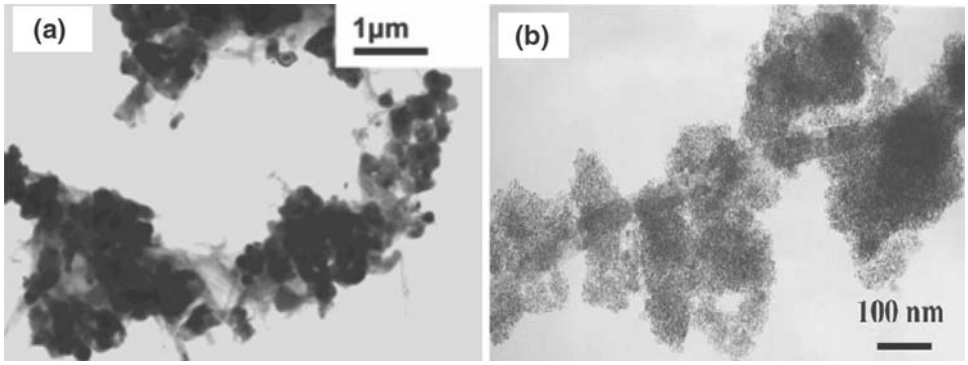

Fig. 5 TEM images of adsorption of **a** Al_2O_3 [77] and **b** TiO_2 [79] nanoparticles on single CNTs during heterocoagulation by colloidal processing. Images published with permission of (**a**) American Chemical Society (ACS) Publications and (**b**) Elsevier B.V.

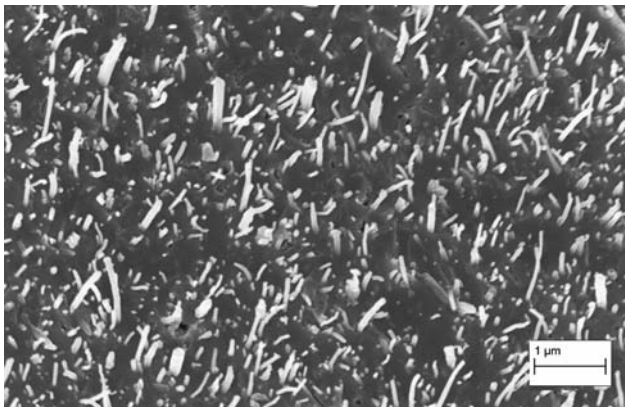

Fig. 6 SEM image showing pull-out of individual CNT (15 wt%) on the fracture surface of SiO_2 glass matrix composites produced by colloidal heterocoagulation and spark-plasma sintering (J. Cho, Unpublished research)

surface properties during the processing phase. However, the CNT/matrix interaction in the resulting composites is likely to vary significantly; the measurement of the interfacial adhesion and its influence on composite properties have not yet been reported.

Sol-gel processing

Sol-gel processing methods provide an alternative route to creating an intimate dispersion of CNTs in inorganic matrices; here, the CNTs are dispersed in a molecular precursor (solution) which then undergoes a condensation reaction to generate a green body for subsequent consolidation. Work to date, has focused mainly on CNTs in silicate sol-gel systems [38, 95–104]. Seeger et al. [38, 95] prepared a 2.5 wt% MWCNT/SiO_2 gel by mixing MWCNTs, acidified water (catalysts) and tetraethoxysilane (TEOS) (silicate precursor), before sintering at 1,150 °C in argon. However, the sintering process led to a partial devitrification of the silica matrix resulting in a heterogeneous microstructure. The use of an alternative sintering method, based on rapid heating of SiO_2/CNT mixtures with a Nd:YAG laser, yielded more homogeneous, fully amorphous silica matrix composites, containing 2.5 wt% MWCNTs [97]. The same method was used by DiMaio et al. [98] to produce silica composites for non-linear optic applications with low CNT content (0.25 wt%). Although, in principle, sol-gel reactions ought to provide a route to good dispersions, agglomeration in the precursor suspensions has proved problematic. Recent work has shown that surface modification of CNTs with organosilanes can stabilise the reaction mixture, leading to excellent CNT dispersion in silicate matrices after consolidation for concentrations of up to 3 wt% MWCNTs [99], as shown in Fig. 7.

The sol-gel method has also been used to synthesize well-dispersed discrete composite rods of CNTs coated with a thin layer of silica [38, 80, 81], titania [84] and alumina [105]. Hwang et al. [80] have developed CNT/SiO_2 composite rods as reinforcing elements for CMCs. In principle, the approach provides a means of modifying the wettability and/or adhesion between CNTs and a chosen ceramic matrix, even after high-temperature consolidation. Although the idea remains to be explored in detail, coatings of sol-gel silica on CNTs have been shown to improve the mixing quality of the CNTs with borosilicate glass powder [63], and to provide a degree of thermal oxidation resistance even at 1,200 °C in air [38].

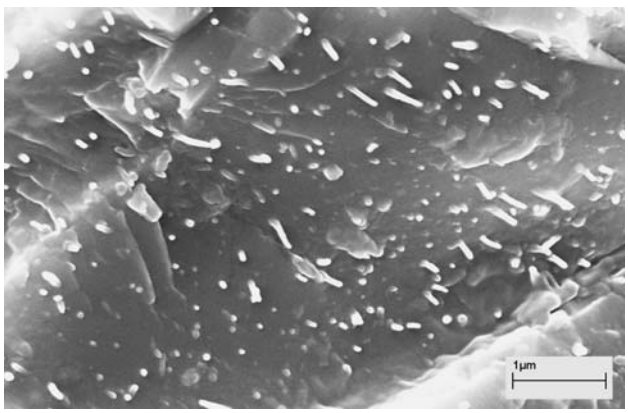

Fig. 7 SEM image of the fracture surface of a MWCNTs/borosilicate glass composites produced by a sol-gel method [99]

Electrophoretic deposition

Electrophoretic deposition (EPD) is a traditional ceramic processing method that is gaining increasing interest as a simple and versatile processing technique for the production of coatings and films from nanoparticles and CNTs [106]. The technique allows the application of coatings of varying thickness to complex 3D shapes including the interior of porous substrates. EPD is achieved via the motion of charged particles, dispersed in a suitable solvent or aqueous solution, towards an electrode under an applied electric field; deposition on the electrode occurs via particle coagulation. Electrophoretic motion of charged particles during EPD results in the accumulation of particles and the formation of a homogeneous and rigid deposit at the relevant electrode [106]. The charge of the suspended particles can be modified by chemical reactions (such as oxidation), the use of surfactants and the adsorption of ions. Comprehensive reviews specifically on EPD of inorganic nanoparticles and CNTs have been published recently [107, 108]. The process of co-depositing a uniform mixture of CNTs and ceramic nanoparticles is shown schematically in Fig. 8. In fact, CNT/ceramic composite layers can be formed by both sequential deposition and co-deposition from mixed suspensions. Chicatun et al. [109] used both approaches to prepare CNT/SiO_2 composite films for possible applications as porous coatings in the biomedical field and as thermal management devices. With appropriate surface modification, the CNTs were efficiently mixed with silica nanoparticles to form a composite CNT/SiO_2 network structure. A similar strategy was used to fabricate four-layer CNT/TiO_2 laminate composite coatings by sequential EPD [110]. Microscopic studies of unsintered materials suggest that the CNT layer can act to reinforce ceramic coatings by providing a crack deflection and delamination path as depicted in Fig. 9a [110]. EPD has been used to generate CNT/bioceramic composites based on hydroxyapatite [111–113] and bioactive glass [114, 115] as well as more device-oriented systems based on combining CNTs with nanocrystals, e.g. Fe_3O_4 [116]. Figure 9b shows a cross-sectional SEM image of Fe_3O_4 nanocrystal film deposited between two CNT mats using the EPD technique [116].

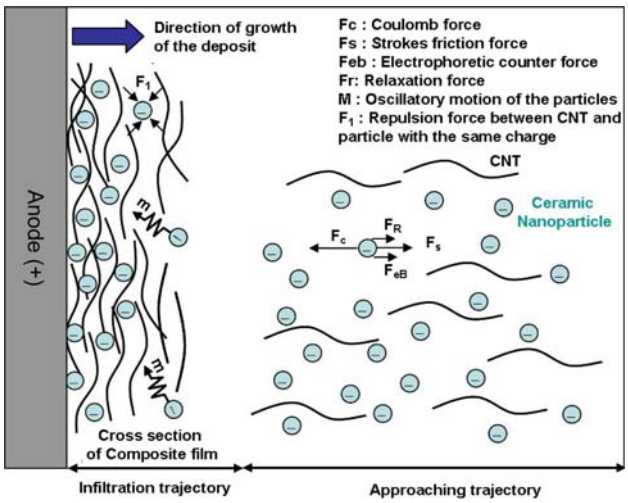

Fig. 8 Schematic illustration of the electrophoretic co-deposition of composite films containing CNTs and ceramic nanoparticles [110]

Advanced consolidation techniques

Due to the high temperatures and long durations involved in conventional pressureless sintering, HPS and hot-isostatic pressing (HIP) methods, degradation of the CNTs during densification of inorganic matrix has often been reported [33, 41, 45, 48, 50, 73, 79–82, 85]. The difficulty of entirely excluding oxygen, or indeed reactions with the matrix or associated impurities, often leads to the loss of the carbonaceous nanotubes. Although these effects can be mitigated by fully coating the CNTs with an inorganic layer before sintering, particularly using sol-gel techniques, some carbon loss is usually experienced. One promising solution that is growing in popularity is the use of a relatively new sintering technique named spark-plasma sintering (SPS) [117]. This technique relies on pulsed DC current passing directly through the powder compact to generate a very high heating and cooling rate (up to 600 °C/min) within the die. The method contrasts with conventional hot-pressing in which the heat is provided by external elements [117]. SPS allows ceramic powders to be

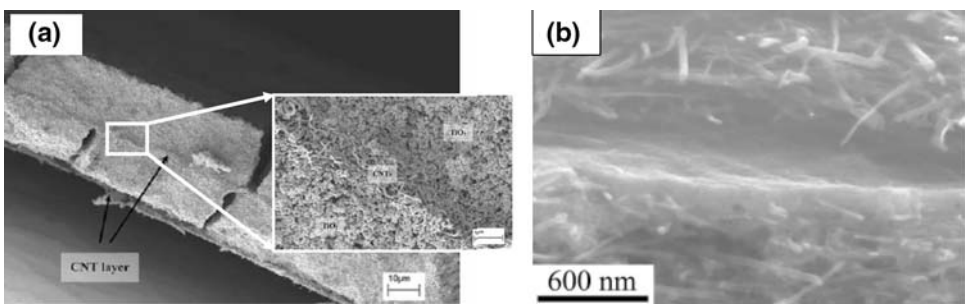

Fig. 9 SEM images showing the cross-section of **a** a four-layer CNT/TiO_2 composite coating produced by sequential electrophoretic deposition [110], and **b** a Fe_3O_4 nanocrystal film between two CNT layers [116]. Images published with permission of (**a**) Springer and (**b**) IOP Publishing Ltd.

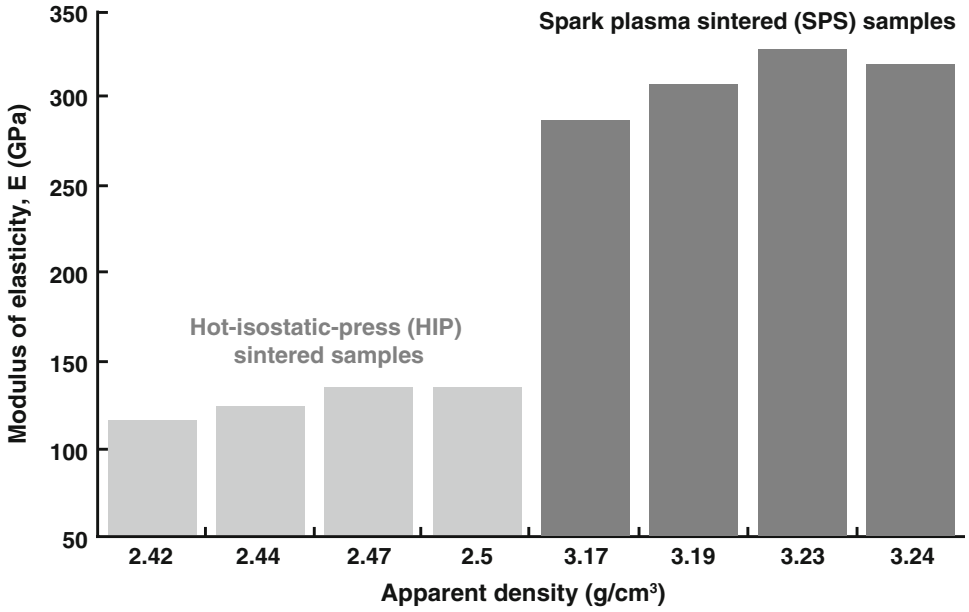

Fig. 10 Modulus of elasticity of composites as a function of apparent density for Si_3N_4 composites containing 6 wt% MWNT produced by hot-isostatic press sintering and spark-plasma sintering [66]. The results clearly indicate that spark-plasma sintering produces highly dense composites leading to at least 100% increase in modulus of elasticity

sintered at lower temperatures and for much shorter times than other sintering processes, and provides a means to control the kinetics of the various processes (densification, chemical reaction and grain growth) that are usually involved during the entire sintering cycle. The short sintering time and low temperatures help to minimise grain growth and offer higher cost-effectiveness and productivity. They also minimise CNT loss, leading to a remarkable improvement in the mechanical properties of eventual CNT/ceramic composites.

Balazsi et al. [66] compared the effectiveness of SPS to conventional HIP for silicon nitride composites reinforced with 6 wt% MWNTs. As can be seen in Fig. 10, fully dense samples with improved mechanical properties were achieved at comparatively lower sintering temperatures by using SPS [66]. The effectiveness of SPS is not only that samples are fully densified, but also that CNTs are retained in the composites. Samples with higher densities showed higher modulus as well as higher hardness and fracture toughness. Similar results have been obtained on introducing SWCNTs into alumina by SPS [70, 71]; apparently undamaged CNTs were incorporated at the grain boundaries, resulting in improved fracture toughness and bending strength (although see below for discussion).

Mechanical properties and possible toughening mechanisms

Table 1 summarises the mechanical properties of CNT/inorganic matrix composites reported in the literature, including a number of significant improvements achieved by addition of CNTs. Most of these studies ultimately aim to increase the fracture toughness; for example, Zhan et al. [71] claimed that the fracture toughness in 10 wt% SWCNTs/Al_2O_3 composites was almost three times higher than that of monolithic alumina, whilst Berguiga et al. [102] reported surprisingly large increases (54% and 69%) for transparent silica composites containing very low loadings (0.025 and 0.05 wt%) of CNTs. Qualitatively, many reports [77, 81, 82] have observed CNT pull-out and crack bridging as toughening mechanisms, using SEM. Quantitatively, due to the small sample volumes available, the majority of researchers have chosen to measure fracture toughness (K_{IC}) using the micro-hardness indentation method, using the following equation: [118]:

$$K_{IC} = \alpha\left(\frac{E}{H}\right)^{1/2} \cdot \left(\frac{P}{C^{3/2}}\right)$$

where E and H are Young's modulus and hardness, respectively, P is the applied load, c is the radial crack length, and α is an empirical constant which depends on the geometry of the indenter. For a cube-corner indenter $\alpha = 0.04$ and for a Vickers indenter $\alpha = 0.016$ [118]. The basic concept is that the crack length at a given load is an indication of the toughness of the tested material (shorter cracks occur in tougher materials).

Results from Wang et al. [119] have, however, questioned the validity of this method for K_{IC} measurements in CNT/ceramic composites. They carried out a comparative investigation with previous results obtained by Zhan et al. [71], using a similar SPS methodology to prepare 10 vol.% SWNT/alumina and control graphite/alumina composites. They pointed out that the Vickers indentation technique is an indirect method for measuring K_{1C}, and that the validity of the fracture toughness results depends critically on the

Table 1 Overview of mechanical properties of CNT/inorganic matrix composites as reported in the literature

Matrix material	CNT content	Processing routes	Investigated properties (%) indicates property improvement compared to monolith	Year
Al_2O_3	SWNT 0.1 wt%	Colloidal processing	Fracture toughness (VI): 4.9 MPa $m^{1/2}$ (31%)	2002 [77]
Al_2O_3	SWNT 10 vol.%	Powder processing	Fracture toughness (VI): 9.7 MPa $m^{1/2}$ (200%)	2002 [71]
Al_2O_3	SWNT 10 vol.%	Powder processing	Fracture toughness (SENB): 3.33 MPa $m^{1/2}$ (3%)	2002 [119]
Al_2O_3	MWNT 4 vol.%	Powder processing	Friction coefficient: 0.45 (−10%), Wear loss: 2 MPa $m^{1/2}$ (−45%)	2003 [49]
Al_2O_3	MWNT 1.5–3.3 vol.%	Sol-gel	Fracture toughness (VI): 1.1 MPa $m^{1/2}$ (10%) with 1.5 wt%	2005 [151]
Al_2O_3	MWNT 1 wt%	Colloidal processing	Bending strength: (10%)	2005 [78]
Al_2O_3	MWNT 12 vol.%	Colloidal processing	Fracture toughness (SENB): 5.55 MPa $m^{1/2}$ (80%)	2006 [82]
Al_2O_3	MWNT 2 wt%	Colloidal processing	Fracture toughness (SENB): = dir. 4.66 MPa $m^{1/2}$ (23.2%), ⊥ dir. 3.65 MPa $m^{1/2}$ (−3.4%)	2007 [125]
			Bending strength: = dir. 390.7 MPa (22%), ⊥ dir. 191 MPa (−36.75%)	
Al_2O_3	SWNT 10 vol.%	Powder processing	Fracture toughness (VI): 9.71 MPa $m^{1/2}$ (200%), Hardness: 1610 kg/mm^2	2007 [122]
Al_2O_3	MWNT 0.9 vol.%	Colloidal processing	Fracture toughness (SENB): 5.9 MPa $m^{1/2}$ (25%), (VI): 6.64 MPa (41%), Bending strength: 689.6 MPa (27%)	2008 [90]
Al_2O_3	MWNT 7 vol.%	Powder processing	Fracture toughness (SENB): 6.8 MPa $m^{1/2}$ (117%), Bending strength: 490 MPa (44%)	2008 [127]
Al_2O_3	MWNT 0.5 wt%	Colloidal processing	Fracture toughness (SENB): 4.8 MPa $m^{1/2}$ (20%), Flexural strength: 572 MPa (17%)	2008 [91]
Al_2O_3	MWNT 3 vol.%	Colloidal processing	Fracture toughness (SENB): 5.01 MPa $m^{1/2}$ (79%), Bending strength: 410 (13%)	2008 [126]
Al_2O_3	MWNT 0.5 wt%	In situ CVD	Fracture toughness (VI): 4.62 MPa $m^{1/2}$ (12%), Hardness: $905.9V_H$ (12%)	2008 [152]
Al_2O_3	MWNT 3.5 vol.%	Colloidal processing	Fracture toughness (VI): 5.2 MPa $m^{1/2}$ (99.5%)	2008 [87]
Al_2O_3	MWNT 10 vol.%	In situ CVD	Frictional coefficient: 0.073 (−50%)	2008 [53]
SiC	MWNT 1–5 vol.%	Sol-gel method	Fracture toughness (VI): 5.4 MPa $m^{1/2}$ (12.5%), Hardness: 30.6 GPa (20%) with 5 vol.%	2007 [56]
Si_3N_4	MWNT 1 wt%	Powder processing	Bending strength: (37%)	2003 [64]
Si_3N_4	MWNT 1–5 vol.%	Colloidal processing	Decrease in both modulus and strength	2006 [67]
Si–C–N	MWNT 1–2 wt%	Colloidal processing	Fracture toughness (SENB): 1.8 MPa $m^{1/2}$ (60%) with 2 wt%	2006 [128]
Mullite	MWNT 5 vol.%	Powder processing	Fracture toughness (VI): (78%), Bending strength: (10%)	2007 [72]
BAS	MWNT 10 vol.%	Powder processing	Fracture toughness (SENB): 2.97 MPa $m^{1/2}$ (140%), Flexural strength: 245 MPa (190%)	2006 [129]
SiO_2	MWNT 6 wt%	Sol-gel method	Hardness: $350H_v$ (100%)	2001 [80]
SiO_2	MWNT 5–30 vol.%	Powder processing	Fracture toughness (VI): 2 MPa $m^{1/2}$ (100%), Bending strength: 85 MPa (65%) with 5 vol.%	2003 [73]
SiO_2	MWNT 5 vol.%	Colloidal processing	Fracture toughness (VI): 2.46 MPa $m^{1/2}$ (146%), Bending strength: 97 MPa (88%)	2004 [81]
SiO_2	MWNT 10 vol.%	Colloidal processing	Fracture toughness (VI): 2.74 MPa (158%), Young's modulus: 43.89 MPa (38%)	2007 [92]
SiO_2	SWNT 0.05 wt%	Sol-gel method	Fracture toughness (VI): 1.05 MPa (69%)	2008 [104]
SiO_2	MWNT 5 vol.%	Colloidal processing	Work of fracture: 0.32 MPa (53%), Compressive strength: 6.1 MPa (33%)	2008 [103]

VI: Vickers Indentation, SENB: single edge notched beam. Where a range of samples have been measured, the sample with the greatest improvement is included in the property column

elastic/inelastic contact-mechanical response of the material under test. They suggest that carbon additions may allow shear deformation under the indenter, as observed by the same group in their previous publication [51]. This accommodation of the deformation may limit the cracking around the indentation, resulting in artificially high fracture toughness values. In the experiments, minor cracking occurred upon indentation but without the classical radial cracks required for the valid K_{1C} measurement [119, 120]. These authors, therefore, questioned the validity of several previous studies in which K_{1C} values had been determined by indentation. Instead, they turned to a macroscopic method for K_{1C} determination, namely the single-edge V-notched beam test (SENB). This test showed virtually no improvement in fracture toughness of the CNT/alumina composites, in contrast to the earlier claims of Zhan et al. [71]. On the other hand, Wang et al's Vickers indentation results [119] do clearly show that SWCNT/alumina composites are highly resistant to contact damage. Although this interpretation is in some senses disappointing, the high resistance to contact damage is, in itself, a very attractive property considering applications such as bearings, valves and other wear resistant machine parts.

A recent comprehensive review of the Vickers indentation method [121] for fracture toughness measurement discusses in detail the limitations of the technique and supports the findings of Wang et al. [119]. It was concluded that the Vickers indentation technique is fundamentally different from other standard fracture toughness tests as the method involves a complex three-dimensional crack system with substantial deformation, residual stress and damage around the cracks. It has been therefore recommended [121] that the method should not be applied to the determination of absolute values of K_{1C} in ceramics but it can still be used to rank materials in terms of their resistance to local damage development (and, of course, hardness and stiffness). Its advantages include simple sample preparation and test operation, low material demands and high speed; given the small size of CNTs, a well-dispersed composite system should give a uniform set of data despite the micron-scale of the indentation.

Recently, there has been an exchange of communications [122–124] continuing the debate on the appropriateness of different fracture toughness measurement techniques for CNT/inorganic matrix composites. Potential problems associated with both the Vickers indentation and the single-edge V-notched beam methods are highlighted, and these discussions may prove interesting to readers engaged in advancing CNT/inorganic matrix composites. Interestingly, in the last 2 years, an increasing number of reports in literature have used the single-edge notch beam method to measure the fracture toughness of various CNT-based systems, including Al_2O_3 [82, 90, 91, 125, 126], hybrid (MWCNTs and SiC nanoparticles/Al_2O_3) [127], Si–C–N [128] and barium aluminosilicate glass–ceramic matrices [129]. This shift may reflect not only the discussions of validity, but also the advancement of SPS methods able to produce the larger quantities of composite required. Nevertheless, effective use of the SENB test requires careful surface preparation and notching; uniform standards are not always reported or applied, possibly still due to material constraints, as specimens of volume of at least 600 mm^3 (e.g. test bars of 3 × 4 mm^2 and length of 50 mm) would be ideally required for statistical meaningful results. A summary of the strength and toughness data presented in Table 1 is plotted in Fig. 11. The increasing performance with CNT loading fraction is clearly highlighted, as is the experimental variability. Other than the examples already discussed, the scatter masks any systematic variation between the Vicker's and SENB data, at present.

Many of the more recent SENB studies continue to suggest improvements in toughness, although at a more modest level than the original Zhan paper [71]. Yamamoto et al. [90], for example, compared SENB and indentation measurements on 0.9 vol.% acid-treated MWCNT/alumina composites produced by SPS. They observed classical radial cracks and CNTs crack-bridging. However, the indentation

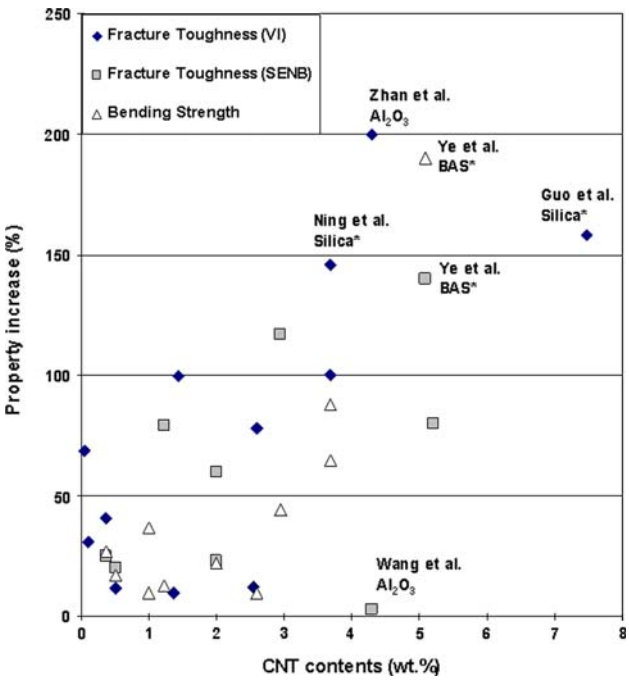

Fig. 11 Summary plot showing the relative (%) increase in fracture toughness, as measured by Vicker's indentation (VI) and Single Edge-Notched Beam (SENB) methods, and bend strength. Volume fractions have been converted to weight fractions assuming a nanotube density of 1.6 g/cc. The named data points are discussed in detail in the text; the asterisks indicate that the addition of nanotubes is known to be associated with a significant change in matrix crystallinity

toughness was significantly higher at 6.64 MPa $m^{1/2}$ (+41%) than the SENB value of 5.90 MPa $m^{1/2}$ (+25%). However, the reasons for this discrepancy were not discussed by the authors [90]. The small number of samples, and especially the small range of, or even single, loading fraction used in the majority of these studies, makes it difficult to isolate the effects of the nanotubes from changes in microstructure or processing. The problem may be particularly acute in glass–ceramics where nucleation effects are likely to be important. Ye et al. [129] reported large mechanical improvements in 10 vol% CNT/barium aluminosilicate glass–ceramic composites which they attributed to crack deflection and pullout. The flexural strength and fracture toughness (measured by SENB) were enhanced by 192% and 143%, respectively, much larger values than achieved with the same content of conventional SiC whiskers, SiC platelets or short carbon fibres. However, changes in degree of crystallinity, crystallite size or orientation were not considered. Similar problems are accounted with polycrystalline ceramics, where for example the location of CNTs, e.g. at grain boundaries or within grains, as well as the effect of CNT on grain growth make difficult to interpret 'true' toughening strength of the CNTs.

For these reasons, the effect of CNTs on glass matrices is particularly interesting, since microstructural variations associated with grain size, orientation and boundaries are avoided. Unfortunately, there are relatively few such studies available [33, 34, 63, 73, 81, 92, 99, 102, 103]. One of the first reports, by Ning et al. [73], looked at powder-processed 5 vol.% MWCNT/SiO_2 composites and claimed significant improvements in fracture toughness (measured by indentation method) (100%) and bending strength (65%). The use of surfactant assisted sol-gel methods allowed Ning et al. [81] subsequently to improve the densification of the composites leading to 146% and 88% increases in fracture toughness (measured by indentation method) and bending strength, respectively. However, the data are surprising given that their SEM images showed large agglomerates of CNTs rather than clear evidence of individual CNT pull-out [81]; the results may relate, at least in part, to a significant degree of matrix crystallisation that was observed. The variable density and crystallinity of the samples, as well as the indentation methodology used, cast some doubt on the significance of the mechanical properties obtained. Similarly processed samples [33, 63] of borosilicate composites with inhomogenous CNT dispersion typically exhibit poor mechanical properties. One difficulty with such amorphous systems is that the glassy matrix may unintentionally crystallise. Indeed, the role of matrix crystallinity in the systems reported to have the greatest increases in toughness is highlighted in Fig. 11. Colloidally processed MWNT/silca composites [92], fully densified by SPS, were found to contain variable fractions of crystalline SiO_2 (cristobalite) despite the lower sintering temperature (950–1,050 °C) and shorter dwell time (5–10 min) compared to conventional hot-pressing. In this case, it is difficult to interpret the increases in Young's modulus and fracture toughness (measured by indentation method) of 40% (60.51GPa) and 160% (2.74 MPa $m^{1/2}$), respectively for the 10 vol% CNT system [92]. In contrast, borosilicate glass composites containing modified-MWNTs, produced using a sol-gel method, were sintered at lower temperatures without inducing crystallisation (see Fig. 7) [99]. A high quality CNT dispersion was maintained at loading fractions below 3 wt%, by using a siloxane coupling agent, and correlated with modest improvements in strength, stiffness and thermal conductivity; however, properties declined above 3 wt% as agglomeration set-in [99]. As noted in the introduction, this behaviour is quite typical of nanocomposites in general.

As well as direct mechanical enhancement of strength, stiffness or toughness, a number of workers have investigated the tribological properties of CNT/CMCs. An et al. [49] fabricated MWCNTs/alumina composites by CVD in situ growth and hot-pressing. It was shown that microhardness increases with increasing CNT content up to 4 wt% whilst the wear loss decreases; however, further additions of CNTs negatively affect both hardness and wear resistance. The tendency for the improvements to be limited to low loading fractions is a familiar phenomenon in both CNT/polymer systems and nanocomposites more widely. The reason is usually the onset of agglomeration as it becomes increasingly difficult for the matrix to cover the high surface area introduced by the nanofiller; alternatively, initial improvements can be associated with changes in the matrix microstructure that do not scale with the introduction of additional filler material [27]. In the work of An et al. [49] the improved wear properties were attributed to the increase in hardness and a decrease in friction coefficient, due to the lubricating properties of the CNTs. The lubrication may arise both from the graphitic nature of the CNTs (and their debris) and, potentially, from the rolling of CNTs at the interface between the specimen and the ball (counter body). On the other hand, the increase in hardness was related mainly to a reduction of the matrix grain size with the inclusion of CNTs. This observation highlights the common difficulty of separating the intrinsic effects due to the presence of CNTs from the processing-related changes in matrix microstructure that they induce. The influence on processing often dominates over any intrinsic mechanical effects, due to the relatively modest loading fractions accessible in well-dispersed systems. Low CNT volume fractions have relatively little impact on average properties, but the associated high surface area, network-forming behaviour and often heterogeneous distribution at grain boundaries can strongly influence

processing issues relating to viscosity, nucleation and grain-boundary effects. Work on sol-gel derived glasses [99] avoids some of these issues and does indicate improvements in stiffness and hardness due to the presence of low loadings of well-dispersed CNTs; however, the effects once again saturate, as CNT agglomeration starts at around 3 wt% loadings.

Several tribological studies have been conducted on thin CNT/ceramic bulk composite and coatings. An aligned MWCNTs/alumina composite was investigated by Xia et al. [53]. In addition to the lubricating nature of CNTs, their work demonstrated that the frictional coefficient of the composites depended on the contact and buckling behaviour of the CNTs by showing that composites with thicker CNTs are more robust to lateral buckling or collapse of the nanotubes. In separate investigations based on scratch testing in physiological solution [130, 131], CNT-reinforced hydroxyapatite coatings exhibited improved wear resistance and lower friction coefficient with increasing CNT loadings (up to 20 wt%). These composites may find potential application as coatings for metal biomedical implants under high load-bearing conditions.

Creep tests of SWCNT/alumina composites have been conducted in uniaxial compression at 1,300 and 1,350 °C in argon; the composites were found to be about two orders of magnitude more creep-resistant than a pure alumina control with about the same grain size ($\sim$0.5 μm) [132]. This improvement is attributed to partial blocking of grain-boundary sliding by SWCNTs in the composites, which is the dominant creep deformation mechanism in monolithic alumina.

Overall, this review of the literature indicates that research focussing on the mechanical performance of CNT/inorganic matrix composites is at a relatively early stage; the reports of modest improvements in mechanical properties do not, for the most part, provide clear evidence linking the quantitative performance data to the actual mechanisms involved. For toughening, CNT pull-out is often claimed as the energy-dissipating mechanisms, but SEM images usually show relatively few CNTs emerging from the composite fracture surfaces. Further work relating properties to mechanism is clearly required; in the meantime it is interesting to consider how traditional toughening mechanisms may scale as the fibre diameter shrinks into the nanoscale.

Assuming that standard short fibre theory applies, the energy absorbed by pulling out one fibre (ΔU) is given by [133]:

$$\Delta U = \pi r L^2 \tau_i^*$$

where r is the fibre radius, L is the fibre length and τ_i^* is the sliding shear stress.

Multiplying by the number of fibres per unit area ($N = V_f/\pi r^2$), and taking the interfacial shear strength as the limit of the sliding shear stress (τ_i^*), gives an approximate upper estimate of the pull-out contribution as:

$$G_{\text{pull-out}} = \frac{V_f L^2 \tau_i}{r}$$

Taking reasonable values based on existing systems, V_f (fibre volume fraction) = 10%, L = 100 nm, r = 10 nm, and τ_i = 10 MPa [134], an estimate for the toughening of 1 Jm^{-2} is obtained. This figure remains relatively small, even if higher loading fractions could be achieved. Similarly, an upper estimate of the energy absorbed in debonding can be obtained from

$$G_{\text{debond}} = 2\pi r L G_i N = \frac{2 V_f L G_i}{r}$$

where G_i is the work of creating the new interface and it is of the order of 4 Jm^{-2} for inorganic matrices [134]; the result, using the parameters above, is only 8 Jm^{-2}. Thus the potential contribution of these two mechanisms appears to be relatively modest; however, this simple model is probably too pessimistic. The use of more perfect nanotubes, with higher strength and/or smaller diameters, might significantly increase the pull-out length, raising the toughening effect. In addition, a variety of additional toughening mechanisms exist such as CNT bridging, CNT buckling/matrix shear [51], as well as the additional deformation and/or friction associated with the pull-out of the intrinsically wavy CNTs. It is worth noting that many CNTs are pulled-out even if not perpendicularly oriented to the crack plane.

The situation is neatly summarised by the model nanocomposites of Xia et al. [51] (discussed in the section "In situ growth of CNTs by chemical vapour decomposition (CVD)", and shown in Fig. 12), which demonstrated the three hallmarks of toughening found in micron-scale fibre reinforced ceramic composites: crack deflection at the CNT/matrix interface, crack bridging by CNTs and CNT pullout on the fracture surfaces. Most interestingly, they also show a number of additional potential toughening mechanisms, associated with shear deformation of the regular array of pores/hollow tubes. However, presumably due to the limited thickness (30 μm) of the templates available, quantitative results of fracture toughness or bending strength are not yet available.

Functional properties of CNT-ceramic matrix composites

In view of the outstanding thermal and electrical properties of CNTs, there have been several investigations focussing on the functional properties of CNT-reinforced inorganic matrix composites, including electrical and thermal

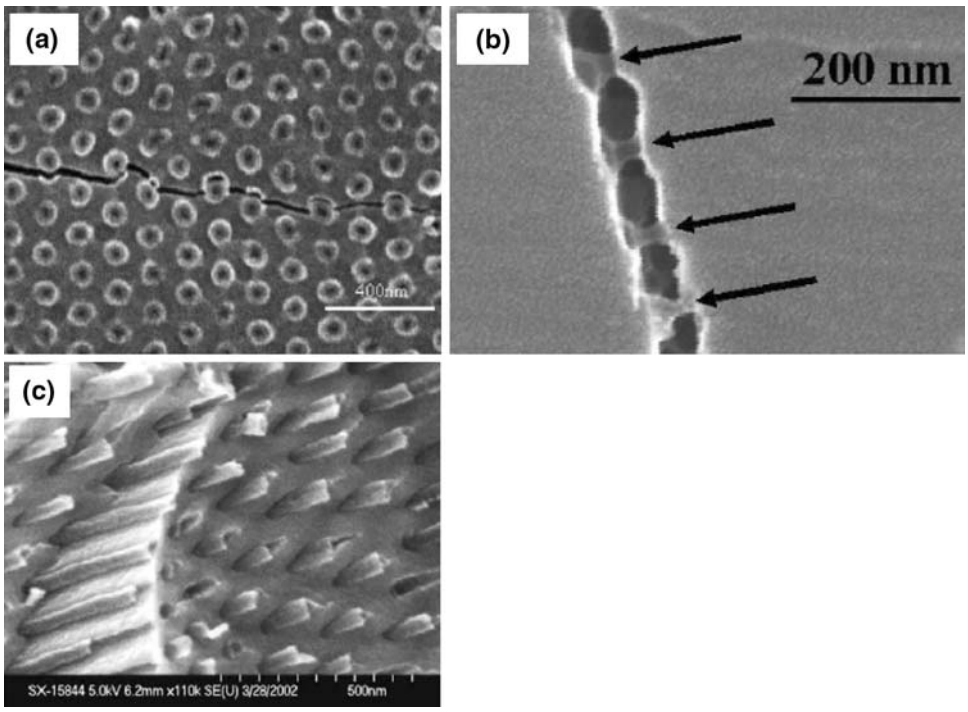

Fig. 12 SEM images showing different failure mechanisms including **a** crack deflection, **b** CNT bridging, **c** CNT pull-out in CNT/alumina composites produced by in situ CVD technique followed by hot-press sintering [51]. Images published with permission of Elsevier B.V.

conductivity. A summary of these results is presented in Table 2. Percolation theory relates a sudden change in a macroscopic property (such as electrical conductivity) to the development of a continuous network structure, at a critical percolation threshold. Around the threshold, the property (e.g. electrical conductivity) can be related to the concentration by a scaling law such as:

$$\sigma_c = \sigma_0(\phi - \phi_c)^t \text{ for } \phi > \phi_c$$

where σ_c is the conductivity of the composite, ϕ is the volume fraction of CNTs in the composite, ϕ_c is the critical volume fraction or percolation threshold and σ_0 and t are fitted constants related to the intrinsic electrical conductivity of the CNTs and the dimensionality of the system, respectively [135].

Electrical percolation of CNTs in an electrical insulating ceramic was studied for the first time by Rul et al. [48]. They reported that the DC electric conductivity of SWCNT/$MgAl_2O_4$ composites (CNT content up to 11 vol.%) was well fitted by the percolation relation with a threshold of 0.64 vol.%, where the conductivity abruptly increased over seven orders of magnitude (from 10^{-10} to 0.0040 S/cm), eventually reaching a maximum at 8.5 S/cm. The electrical conductivities of a variety of other inorganic matrix materials containing MWCNTs have been measured, including SiC [56], TiN [57], Fe_2 N [57], borosilicate glass [99], SiO_2 [93] ZrO_2 [136, 137] and Si_3N_3 [138] systems. The thresholds on the order of 1 vol.% are typical of a large number of CNT/polymer composite systems and are in line with expectations from excluded volume considerations; in other words, the high aspect ratio of the CNTs gives rise to a large hydrodynamic volume and effective statistical network formation. Much lower percolation thresholds have been observed but are associated with kinetically driven network formation or phase segregation [36]; in this context, poor CNT distribution or dispersion can provide lower percolation thresholds.

Absolute values of the electrical conductivity are typically well above the level needed for static dissipation and approach the level needed for electromagnetic shielding applications. One of the highest absolute conductivities (33 S/cm) was achieved in dense alumina composites containing up to 15 vol.% SWCNTs fabricated by spark-plasma-sintering [70]. Electromagnetic interference (EMI) shielding properties of MWCNTs reinforced fused silica composites have been investigated in the frequency region 36.5–40 GHz (K_a band) [139]. Shielding improved with MWNT content reaching 68 dB for the 10 vol.% sample at 36–37 GHz, indicating a possible commercial application at relevant high frequencies. The EMI shielding effectiveness of an equivalent carbon black-fused silica composite saturated at high frequencies. Indeed, for a given loading fraction, the electrical conductivity of CNT-loaded systems tends to be one to two orders of magnitude higher than that of carbon black composites, due to the higher intrinsic conductivity of CNTs and the much higher connectivity of the network.

Table 2 Overview of functional properties of CNT/inorganic matrix composites as reported in the literature

Matrix material	CNT contents	Processing routes	Investigated properties (%) indicates property improvement compared to monolith	Year
Fe/Co-$MgAl_2O_4$	–	In situ CVD	Electrical conductivity: extrusion direction 20 S/cm, transverse direction 0.6 S/cm	2002 [45]
$MgAl_2O_4$	0.2–25 vol.%	In situ CVD	Percolation threshold at 0.64 vol.% CNTs	2004 [48]
Al_2O_3	SWNT 5.7–15 vol.%	Powder processing	Electrical conductivity: 3345 S/m with 15 vol.% CNTs	2003 [70]
Al_2O_3	MWNT 2 wt%	Colloidal processing	Electrical conductivity: = dir. 6.2×10^{-2} S/m, $\perp$ dir. 6.8×10^{-9} S/m	2007 [125]
Al_2O_3	MWNT 4.65 vol.%	Colloidal processing	Electrical conductivity: 210 S/m	2008 [89]
TiO_2	MWNT 1.5 wt%	Colloidal processing	Photocatalytic properties in Phenol degradation	2003 [79]
TiN	12.4 vol%	In situ CVD	Electrical conductivity: 735 S/cm (44.7%)	2005 [57]
Fe_2 N	11.7 vol.%	In situ CVD	Electrical conductivity: 885 S/cm (11.5%)	2005 [57]
Si_3N_4	1.8–12 wt%	Colloidal processing	Electrical conductivity: 79 S/m with 1.8 wt% CNT	2005 [138]
SiC	0.3–2.1 vol.%	In situ CVD	Electrical resistivity: (− 96%) at 2.1 vol.% CNTs	2005 [153]
ZrO_2	MWNT 10 wt%	Colloidal processing	Percolation threshold at 1.7 wt% CNT	2006 [137]
SiO_2	MWNT 10 vol.%	Sol-gel	Thermal diffusion coefficient: (16.3%), thermal conductivity: (20.6%)	2003 [141]
SiO_2	MWNT 10 vol.%	Colloidal processing	Electromagnetic interference shielding: 69 dB with 10 vol% CNTs	2007 [139]
SiO_2	MWNT 10 vol.%	Colloidal processing	Electrical conductivity: 65 S/m	2007 [93]
SiO_2	MWNT 10 vol.%	Colloidal processing	Thermal conductivity: 4.08 W/m K (69%)	2007 [94]

Peigney et al. [45] also investigated anisotropic electrical conductivity in SWCNTs/Fe/Co-$MgAl_2O_4$ composites following extrusion. As expected, the conductivity in parallel direction to the extrusion direction was much higher (by a factor of approximately 30) than that measured in the transverse direction, providing evidence of preferential alignment of the CNTs following extrusion; similar effects are well-known in polymer systems [36]. The anisotropy of the electrical conductivity was also studied in MWCNTs/alumina composites where CNT alignment was induced by DC electric fields [125]. The results showed a difference of about seven orders of magnitude between the electric conductivities in longitudinal (6.2×10^{-2} S/m) and transverse (6.8×10^{-9} S/m) directions. It is worth noting that, for a given aspect ratio, alignment of fibres actually increases the percolation threshold [140].

Relatively few studies have explored thermal conductivity; a strong percolation behaviour is not expected as there are, at most, only two to three orders of magnitude difference between the thermal conductivity of the CNTs and the inorganic matrix.

MWCNTs/SiO_2 composites showed systematic increases in thermal diffusion coefficient and thermal conductivity with increasing CNT content [141]. At 650 °C, the thermal conductivity was enhanced by 20.6% (~2 W/m.K) at 10 vol.% CNTs, compared to that of monolithic SiO_2. More recently, a thermal conductivity of 4.08 W/m.K was measured on fully dense 10 vol.% MWCNTs/SiO_2 composites processed by SPS [94]. In sol-gel derived borosilicate/MWCNTs composites, thermal conductivities of up to 1.45 W/mK were measured at room temperature for composites containing 2 wt% MWCNT (compared to the matrix value of 1.1 W/mK) [99]. Nevertheless, the increases reported are relatively modest compared to the high intrinsic thermal conductivity of CNTs. The relatively small improvements may be due to the high interface thermal resistance [142, 143], and the large interfacial surface area between CNTs and the matrix. It is also worth noting that the intrinsic thermal conductivity of the CVD nanotubes used in composite systems will be lower than the ideal value. Although there may be some improvement during sintering, most inorganic matrices are processed at too low a temperature for large improvements of thermal conductivity due to graphitisation of the CNTs.

Encapsulating CNTs in transparent inorganic glass (or glass-like) matrices may enable or enhance photonic applications, including nonlinear optics, planar optical wave guides, optical switches and optical limiting devices. CNTs have been shown to be broadband optical limiters, efficient at both 532 and 1,064 nm laser wavelength in solutions [15, 144] and polymer composites [145]. Although theoretical calculations show that CNTs have large third-order optical nonlinearities there are relatively

few experimental reports available [98, 100, 146–148]. On the other hand, nanotube arrays and composites have been successfully used as saturable absorbers for mode-locked lasers [149, 150]. In high power situations, inorganic matrices may offer improved stability than current systems. For optical applications, sol-gel techniques are usually employed to produce transparent and structural composites containing low volume fractions of CNTs. Exploiting the desirable optical effects requires a good dispersion of the nanotubes to retain clarity and avoid Rayleigh scattering.

Future work and conclusions

The present review of CNT-reinforced inorganic matrix composites describes the latest processing techniques developed to improve the mechanical and functional properties of CNT-reinforced ceramics and glasses. These techniques have gradually provided better and more consistent properties compared to traditional powder processing methods. However, further improvements in processing techniques are still required in order to develop high quality samples in sufficient quantities for reliable property determination, particularly of fracture toughness. The relationship between the nanocomposite structure, the properties and the active toughening mechanisms remains to be established. Moreover, in order to fully exploit the reinforcing ability of CNTs, it is clear that several critical issues remain to be solved, including: (i) homogeneous dispersion of CNTs in the matrix system, (ii) optimisation of the interfacial bonding between CNTs and adjacent matrix and (iii) development of novel consolidation methods/conditions that do not lead to CNT damage. In addition, higher quality CNTs, with intrinsic properties approaching the theoretical limit, are needed in sufficiently large volumes and purities for application in novel composite systems. The relationship of the toughening mechanisms to the wide variety of structural parameters associated with CNTs must also be established. Systematic studies exploring the impact of CNT dimensions, crystallinity, straightness, entanglement, internal structure and concentration will be needed in order to establish the 'ideal' nanotube for a given system or application.

On the other hand, many argue that the real value of CNTs lies in their range and breadth of properties, which include mechanical, electrical and thermal properties. These properties provide additional benefits when incorporating CNTs in ceramic and glass matrices, which enable the development of multifunctional structural materials with a relatively low concentration of filler. It is worth remembering that the small size of CNTs allows them to be incorporated where conventional fibre reinforcements cannot be accommodated, for example in thin and thick films, coatings, foams and in the matrix of conventional fibre composites. This concept has begun to be exploited in the polymer systems but remains to be explored using inorganic matrices.

References

1. Chawla KK (2003) Ceramic matrix composites, 2nd edn. Springer, New York
2. Sternitzke M (1997) J Eur Ceram Soc 17(9):1061
3. Matthews FL, Rawlings RD (2003) Composite materials: engineering and science. Woodhead Publishing Limited, Cambridge, England
4. Marshall DB, Evans AG (1985) J Am Ceram Soc 68(5):225
5. Brennan JJ, Prewo KM (1982) J Mater Sci 17(8):2371. doi: 10.1007/BF00543747
6. Beyerle DS, Spearing SM, Zok FW, Evans AG (1992) J Am Ceram Soc 75(10):2719
7. Chawla KK (1998) Fibrous materials. Cambridge University Press, Cambridge
8. Bunsell A, Berger M (1999) Fine ceramic fibres. CRC Press, New York
9. Dicarlo JA (1985) J Met 37(6):44
10. Crivelli-Visconti I, Cooper GA (1969) Nature 221:754
11. Evans AG, Zok FW (1994) J Mater Sci 29(15):3857. doi: 10.1007/BF00355946
12. Baughman R (2002) Science's Compas 297(2):787
13. Yu MF, Lourie O, Dyer MJ, Moloni K, Kelly TF, Ruoff RS (2000) Science 287(5453):637
14. Kaneto K, Tsuruta M, Sakai G, Cho WY, Ando Y (1999) Synth Met 103(1–3):2543
15. Riggs JE, Walker DB, Carroll DL, Sun YP (2000) J Phys Chem B 104(30):7071
16. Berber S, Kwon YK, Tomanek D (2000) Phys Rev Lett 84(20): 4613
17. Lau KT, Hui D (2002) Compos Part B-Eng 33(4):263
18. Thostenson ET, Ren ZF, Chou TW (2001) Compos Sci Technol 61(13):1899
19. Sandler JKW, Kirk JE, Kinloch IA, Shaffer MSP, Windle AH (2003) Polymer 44(19):5893
20. Zheng LX, O'Connell MJ, Doorn SK, Liao XZ, Zhao YH, Akhadov EA, Hoffbauer MA, Roop BJ, Jia QX, Dye RC, Peterson DE, Huang SM, Liu J, Zhu YT (2004) Nat Mater 3(10): 673
21. Bethune DS, Kiang CH, Devries MS, Gorman G, Savoy R, Vazquez J, Beyers R (1993) Nature 363(6430):605
22. Ebbesen TW, Ajayan PM (1992) Nature 358(6383):220
23. Thess A, Lee R, Nikolaev P, Dai HJ, Petit P, Robert J, Xu CH, Lee YH, Kim SG, Rinzler AG, Colbert DT, Scuseria GE, Tomanek D, Fischer JE, Smalley RE (1996) Science 273(5274): 483
24. Cheng HM, Li F, Su G, Pan HY, He LL, Sun X, Dresselhaus MS (1998) Appl Phys Lett 72(25):3282
25. Tibbetts GG, Gorkiewicz DW, Alig RL (1993) Carbon 31(5):809
26. Salvetat JP, Kulik AJ, Bonard JM, Briggs GAD, Stockli T, Metenier K, Bonnamy S, Beguin F, Burnham NA, Forro L (1999) Adv Mater 11(2):161
27. Shaffer MSP, Sandler JKW (2006) Processing and properties of nanocomposites. World Scientific, Singapore, pp 1–59
28. Andrews R, Jacques D, Qian DL, Rantell T (2002) Acc Chem Res 35(12):1008
29. Ramirez AP (2005) Bell Labs Tech J 10(3):171
30. Shaffer M, Kinloch IA (2004) Compos Sci Technol 64(15):2281

31. Coleman JN, Khan U, Blau WJ, Gun'ko YK (2006) Carbon 44:1624
32. Dai HJ (2002) Surf Sci 500(1–3):218
33. Boccaccini AR, Acevedo DR, Brusatin G, Colombo P (2005) J Eur Ceram Soc 25(9):1515
34. Arvantelis C, Jayaseelan DD, Cho J, Boccaccini AR (2008) Adv Appl Ceram 107(3):155
35. Harris PJF (2004) Int Mater Rev 49(1):31
36. Kovacs JZ, Velagala BS, Schulte K, Bauhofer W (2007) Compos Sci Technol 67(5):922
37. Qian D, Dickey EC, Andrews R, Rantell T (2000) Appl Phys Lett 76(20):2868
38. Seeger T, Redlich P, Grobert N, Terrones M, Walton DRM, Kroto HW, Ruhle M (2001) Chem Phys Lett 339(1–2):41
39. Peigney A, Laurent C, Dumortier O, Rousset A (1998) J Eur Ceram Soc 18(14):1995
40. Laurent C, Peigney A, Dumortier O, Rousset A (1998) J Eur Ceram Soc 18(14):2005
41. Flahaut E, Peigney A, Laurent C, Marliere C, Chastel F, Rousset A (2000) Acta Mater 48(14):3803
42. Flahaut E, Peigney A, Laurent C, Rousset A (2000) J Mater Chem 10(2):249
43. Flahaut E, Rul S, Lefevre-Schlick F, Laurent C, Peigney A (2004) Ceram Nanomater Nanotechnol II 148:71
44. Peigney A (2003) Nat Mater 2(1):15
45. Peigney A, Flahaut E, Laurent C, Chastel F, Rousset A (2002) Chem Phys Lett 352(1–2):20
46. Peigney A, Laurent C, Flahaut E, Rousset A (2000) Ceram Int 26(6):677
47. Peigney A, Rul S, Lefevre-Schlick F, Laurent C (2007) J Eur Ceram Soc 27(5):2183
48. Rul S, Lefevre-schlick F, Capria E, Laurent C, Peigney A (2004) Acta Mater 52(4):1061
49. An JW, You DH, Lim DS (2003) Wear 255:677
50. Lim DS, You DH, Choi HJ, Lim SH, Jang H (2005) Wear 259(1–6):539
51. Xia Z, Riester L, Curtin WA, Li H, Sheldon BW, Liang J, Chang B, Xu JM (2004) Acta Mater 52(4):931
52. Xia Z, Curtin WA, Sheldon BW (2004) J Eng Mater Technol-Trans ASME 126(3):238
53. Xia ZH, Lou J, Curtin WA (2008) Scripta Mater 58(3):223
54. Kamalakaran R, Lupo F, Grobert N, Lozano-Castello D, Jin-Phillipp NY, Ruhle M (2003) Carbon 41(14):2737
55. Kamalakaran R, Lupo F, Grobert N, Scheu T, Jin-Phillipp NY, Ruhle M (2004) Carbon 42(1):1
56. Morisada Y, Miyamoto Y, Takaura Y, Hirota K, Tamari N (2007) Int J Refract Metal Hard Mater 25(4):322
57. Jiang LQ, Gao L (2005) J Mater Chem 15(2):260
58. Jiang LQ, Gao L (2006) J Am Ceram Soc 89(1):156
59. Huang Q, Gao L (2005) Appl Phys Lett 86:123104
60. Huang Q, Gao L (2004) J Mater Chem 14(16):2536
61. Huang Q, Gao L, Liu YQ, Sun J (2005) J Mater Chem 15(20):1995
62. Huang Q, Gao L, Sun J (2005) J Am Ceram Soc 88(12):3515
63. Boccaccini AR, Thomas BJC, Brusatin G, Colombo P (2007) J Mater Sci 42(6):2030. doi:10.1007/s10853-006-0540-7
64. Balazsi C, Konya Z, Weber F, Biro LP, Arato P (2003) Mater Sci Eng C-Bio Supramol Syst 23(6–8):1133
65. Balazsi C, Weber F, Kover Z, Konya Z, Kiricsi I, Biro LP, Arato P (2005) Fractogr Adv Ceram II 290:135
66. Balazsi C, Shen Z, Konya Z, Kasztovszky Z, Weber F, Vertesy Z, Biro LP, Kiricsi I, Arato P (2005) Compos Sci Technol 65(5):727
67. Balazsi C, Fenyi B, Hegman N, Kover Z, Weber F, Vertesy Z, Konya Z, Kiricsi I, Biro LP, Arato P (2006) Compos Part B-Eng 37(6):418
68. Balazsi C, Weber F, Kover Z, Shen Z, Konya Z, Kasztovszky Z, Vertesy Z, Biro LP, Kiricsi I, Arato P (2006) Curr Appl Phys 6(2):124
69. Balazsi C, Sedlackova K, Czigany Z (2008) Compos Sci Technol 68(6):1596
70. Zhan GD, Kuntz JD, Garay JE, Mukherjee AK (2003) Appl Phys Lett 83(6):1228
71. Zhan GD, Kuntz JD, Wan JL, Mukherjee AK (2003) Nat Mater 2(1):38
72. Wang J, Kou HM, Liu XJ, Pan YB, Guo JK (2007) Ceram Int 33(5):719
73. Ning JW, Zhang JJ, Pan YB, Guo JK (2003) Mater Sci Eng A Struct Mater 357(1–2):392
74. Shaffer MSP, Fan X, Windle AH (1998) Carbon 36(11):1603
75. Poyato R, Vasiliev AL, Padture NP, Tanaka H, Nishimura T (2006) Nanotechnology 17(6):1770
76. Du CS, Yeh J, Pan N (2005) J Mater Chem 15(5):548
77. Sun J, Gao L, Li W (2002) Chem Mater 14(12):5169
78. Sun J, Gao L, Jin XH (2005) Ceram Int 31(6):893
79. Sun J, Gao L (2003) Carbon 41(5):1063
80. Hwang GL, Hwang KC (2001) J Mater Chem 11(6):1722
81. Ning JW, Zhang JJ, Pan YB, Guo JK (2004) Ceram Int 30(1):63
82. Fan JP, Zhao DQ, Wu MS, Xu ZN, Song J (2006) J Am Ceram Soc 89(2):750
83. Moore VC, Strano MS, Haroz EH, Hauge RH, Smalley RE, Schmidt J, Talmon Y (2003) Nano Lett 3(10):1379
84. Sun J, Iwasa M, Gao L, Zhang QH (2004) Carbon 42(4):895
85. Fan JP, Zhao DQ, Xu ZN, Wu MS (2005) Sci China Ser E-Eng Mater Sci 48(6):622
86. Fan JP, Zhuang DM, Zhao DQ, Zhang G, Wu MS, Wei F, Fan ZJ (2006) Appl Phys Lett 89(12):3
87. Estili M, Kawasaki A (2008) Scripta Mater 58(10):906
88. Balani K, Agarwal A (2008) Nanotechnology 19:165701
89. Inam F, Yan H, Reece MJ, Peijs T (2008) Nanotechnology 19:195710
90. Yamamoto G, Omori M, Hashida T, Kimura H (2008) Nanotechnology 19:315708
91. Yamamoto G, Omori M, Hashida T (2008) Water Dynamics 987:83
92. Guo SQ, Sivakumar R, Kagawa Y (2007) Adv Eng Mater 9(1–2):84
93. Guo SQ, Sivakumar R, Kitazawa H, Kagawa Y (2007) J Am Ceram Soc 90(5):1667
94. Sivakumar R, Guo SQ, Nishimura T, Kagawa Y (2007) Scripta Mater 56(4):265
95. Seeger T, Kohler T, Frauenheim T, Grobert N, Ruhle M, Terrones M, Seifert G (2002) Chem Commun 7(1):34
96. Grobert N, Seeger T, Seifert G, Ruhle M (2003) J Ceram Process Res 4(1):1
97. Seeger T, de la Fuente G, Maser WK, Benito AM, Callejas MA, Martinez MT (2003) Nanotechnology 14(2):184
98. DiMaio J, Rhyne S, Ballato J, Czerw R, Xu J, Webster S, Carroll DL, Fu K, Sun YP (2001) Inorg Opt Mater III 4452:48
99. Thomas BC, Shaffer MSP, Boccaccini AR (2008) Composites Part A, submitted
100. de Andrade MJ, Lima MD, Stein L, Bergmann CP, Roth S (2007) Physica Stat Sol B-Basic Solid State Phys 244:4218
101. Zhang YJ, Shen YF, Han DX, Wang ZJ, Song JX, Niu L (2006) J Mater Chem 16(47):4592
102. Berguiga L, Bellessa J, Vocanson F, Bernstein E, Plenet JC (2006) Opt Mater 28(3):167
103. Zheng C, Feng M, Zhen X, Huang J, Zhan HB (2008) J Non-Cryst Solids 354(12–13):1327
104. de Andrede MJ, Lima MD, Bergmann CP, Ramminger GD, Balzaretti NM, Costa TMH, Gallas MR (2008) Nanotechnology 19:265607

105. Hernadi K, Ljubovic E, Seo JW, Forro L (2003) Acta Mater 51(5):1447
106. Boccaccini AR, Zhitomirsky I (2002) Curr Opinion Solid State Mater Sci 6(3):251
107. Corni I, Ryan MP, Boccaccini AR (2008) J Eur Ceram Soc 28(7):1353
108. Boccaccini AR, Cho J, Roether JA, Thomas BJC, Minay EJ, Shaffer MSP (2006) Carbon 44(15):3149
109. Chicatun F, Cho J, Schaab S, Brusatin G, Colombo P, Roether JA, Boccaccini AR (2007) Adv Appl Ceram 106(4):186
110. Cho J, Schaab S, Roether JA, Boccaccini AR (2008) J Nanopart Res 10:99
111. Correa-Duarte MA, Wagner N, Rojas-Chapana J, Morsczeck C, Thie M, Giersig M (2004) Nano Lett 4(11):2233
112. Zhao LP, Gao L (2004) Carbon 42(2):423
113. Aryal S, Bahadur KCR, Dharmaraj N, Kim KW, Kim HY (2006) Scripta Mater 54(2):131
114. Singh I, Kaya C, Shaffer MSP, Thomas BC, Boccaccini AR (2006) J Mater Sci 41(24):8144. doi:10.1007/s10853-006-0170-0
115. Cho J, Cannio M, Boccaccini AR (2009) Int J Mater Product Technol (in press)
116. Mahajan SV, Hasan SA, Cho J, Shaffer MSP, Boccaccini AR, Dickerson JH (2008) Nanotechnology 19:195301
117. Dobedoe RS, West GD, Lewis MH (2005) Adv Appl Ceram 104(3):110
118. Anstis GR, Chantikul P, Lawn BR, Marshall DB (1981) J Am Ceram Soc 64(9):533
119. Wang XT, Padture NP, Tanaka H (2004) Nat Mater 3(8):539
120. Sheldon BW, Curtin WA (2004) Nat Mater 3(8):505
121. Quinn GD, Bradt RC (2007) J Am Ceram Soc 90(3):673
122. Jiang DT, Thomson K, Kuntz JD, Ager JW, Mukherjee AK (2007) Scripta Mater 56(11):959
123. Padture NP, Curtin WA (2008) Scripta Mater 58(11):989
124. Jiang D, Mukherjee AK (2008) Scripta Mater 58(11):991
125. Zhu YF, Shi L, Zhang C, Yang XZ, Liang J (2007) Appl Phys A-Mater Sci Process 89(3):761
126. Wei T, Fan ZJ, Luo GH, Wei F (2008) Mater Lett 62(4–5):641
127. Ahmad K, Pan W (2008) Compos Sci Technol 68(6):1321
128. Katsuda Y, Gerstel P, Narayanan J, Bill J, Aldinger F (2006) J Eur Ceram Soc 26(15):3399
129. Ye F, Liu LM, Wang YJ, Zhou Y, Peng B, Meng QC (2006) Scripta Mater 55(10):911
130. Balani K, Chen Y, Harlinkar SP, Dahotre NB, Agarwal A (2007) Acta Biomater 3(6):944
131. Chen Y, Zhang TH, Gan CH, Yu G (2007) Carbon 45(5):998
132. Zapata-Solvas E, Poyato R, Gomez-Garcia D, Dominguez-Rodriguez A, Radmilovic V, Padture NP (2008) Appl Phys Lett 92:111912
133. Hull D, Clyne TW (1996) An introduction to composite materials. Cambridge University Press, Cambridge
134. Klug T (1994) J Mater Sci 29(15):4013. doi:10.1007/BF00355963
135. Chung DL (2003) Composite materials: functional materials for modern technologies. Springer, New York
136. Shi SL, Liang J (2007) J Appl Phys 101(2):023708
137. Shi SL, Liang J (2006) J Am Ceram Soc 89(11):3533
138. Tatami J, Katashima T, Komeya K, Meguro T, Wakihara T (2005) J Am Ceram Soc 88(10):2889
139. Xiang CS, Pan Y, Guo JK (2007) Ceram Int 33(7):1293
140. Rahatekar SS, Hamm M, Shaffer MSP, Elliott JA (2005) J Chem Phys 123(13):134702
141. Ning JW, Zhang JJ, Pan YB, Guo JK (2003) J Mater Sci Lett 22(14):1019
142. Nan CW, Liu G, Lin YH, Li M (2004) Appl Phys Lett 85(16):3549
143. Nan CW, Shi Z, Lin Y (2003) Chem Phys Lett 375(5–6):666
144. Liu LQ, Zhang SA, Hu TJ, Guo ZX, Ye C, Dai LM, Zhu DB (2002) Chem Phys Lett 359(3–4):191
145. Jin ZX, Sun X, Xu GQ, Goh SH, Ji W (2000) Chem Phys Lett 318(6):505
146. Yim JH, Kim JT, Lee S, Rotermund F, Koh KH (2007) Nonlinear optical properties of SWCNTs incorporated silica composites. 2007 2nd Ieee international conference on nano/micro engineered and molecular systems, vols 1–3, pp 606–610
147. Zhan HB, Zheng C, Chen WZ, Wang MQ (2005) Chem Phys Lett 411(4–6):373
148. Zhan HB, Chen WZ, Wang MQ, Zhengchan, Zou CL (2003) Chem Phys Lett 382(3–4):313
149. Wang F, Rozhin AG, Sun Z, Scardaci V, Penty RV, White IH, Ferrari AC (2008) Int J Mater Form 1(2):107
150. Scardaci V, Rozhin AG, Hennrich F, Milne WI, Ferrari AC (2007) Physica E-Low-Dimen Syst Nanostruct 37(1–2):115
151. Mo CB, Cha SI, Kim KT, Lee KH, Hong SH (2005) Mater Sci Eng A Struct Mater 395(1–2):124
152. Balani K, Zhang T, Karakoti A, Li WZ, Seal S, Agarwal A (2008) Acta Mater 56(3):571
153. Thostenson ET, Karandikar PG, Chou TW (2005) J Phys D-Appl Phys 38(21):3962